Journal of Human, Environment and Health Promotion. 2018; 4(4): 153-158

Journal of Human, Environment and Health Promotion

Journal homepage: www.zums.ac.ir/jhehp

Equilibrium, Isotherm and Kinetic Adsorption Studies of Direct Blue 71 onto Raw Kaolin

Davoud Balarak [a*] | **Mohadeseh Dashtizadeh** [b] | **Mohadeseh Zafariyan** [b] | **Masomeh Sadeghi** [b]

[a] *Department of Environmental Health, Health Promotion Research Center, School of Public Health, Zahedan University of Medical Sciences, Zahedan, Iran.*
[b] *Department of Environmental Health, Student Research Committee, Zahedan University of Medical Sciences, Zahedan, Iran.*

***Corresponding author:** Davoud Balarak
Department of Environmental Health, Health Promotion Research Center, School of Public Health, Zahedan University of Medical Sciences, Zahedan, Iran. Postal Code: 7189785978.
E-mail address: dbalarak2@gmail.com

ARTICLE INFO

Article type:
Original article

Article history:
Received September 30, 2018
Revised November 5, 2018
Accepted November 21, 2018

DOI: 10.29252/jhehp.4.4.2

Keywords:
Direct blue 71 dye
Adsorption isotherms
Kinetic

ABSTARACT

Background: Nowadays, the development of new materials is emergent that can be used in the adsorption process to remove dyes from the aquatic environment. Therefore, in this study, the performance of raw Kaolin as a low cost adsorbent was evaluated in removing Direct Blue 71 (DB71) dye from aqueous solutions.
Methods: For investigating the adsorption, various parameters were optimized and data were adjusted to four isotherm models: Freundlich, Dubinin–Radushkevich, Langmuir and Temkin, in order to determine the one presenting the best adjustment to the experimental data. Moreover, the kinetics study for adsorption was evaluated using diffusion, pseudo-first-order kinetic and pseudo-second-order kinetic models.
Results: The results revealed that at the DB71 concentration of 10 mg/L, adsorbent dose of 2.5 g/L, and contact time of 75 min, the DB71 removal reached 98.5%. Adsorption data fitted best into the Langmuir and D-R adsorption isotherms. The maximum monolayer adsorption capacity was 36.41 mg/g. The pseudo second order kinetics best described the kinetics of the adsorption system.
Conclusion: It was revealed that Kaolin could be applied for DB71 dye removal from solution samples with the adsorption capacity of 36.41 mg/g and thus could be used as a low-cost and effective adsorbent.

1. Introduction

The presence of dyes in wastewater unfortunately causes adverse effects in the marine environment [1, 2]. However, most of the wastewater treatment technologies are not designed for contaminants of emerging treatment [3, 4]. The misuse and less adsorption of dyes lead to high water solubility and persistent behavior that present the worldwide environmental pollution, which, in turn, causes serious health problems [5].

Dyes are widely used in industries such as textiles, leather, printing, food, plastics, etc. The removal of dyes from industrial wastewaters is a major problem [6]. Conventional methods for the removal of dyes from wastewater include adsorption onto solid substrates, chemical coagulation, oxidation, filtration and biological treatment [7, 8].

Adsorption is one of the effective separation techniques to remove organic and inorganic pollutants. Therefore, researches have been continued in pursue of cheaper, easily obtainable materials for the adsorption of dyes [9, 10].

To cite: Balarak D, Dashtizadeh M, Zafariyan M, Sadeghi M. Equilibrium, Isotherm and Kinetic Adsorption Studies of Direct Blue 71 onto Raw Kaolin. *J Hum Environ Health Promot*. 2018; 4(4): 153-8.

Removal of dyes by adsorption has been extensively studied in the last years. Activated carbon has been successfully used in removing colored organic species while it is the most widely used as adsorbent due to its high capacity of adsorption for organic materials [11]. However, due to its high cost, an effective and cheap adsorbent material is still an urgent need [12]. Lately, many local inexpensive materials have been studied as new adsorbents to remove pollutants and dyes from wastewater [13, 14]. The use of low cost adsorbents, such as natural ores, agricultural byproducts and industrial wastes, is preferable. Thus, the important task is to develop and improve adsorbent materials derived from solid wastes [15]. These materials are not expensive and can be used for contaminants treatment like dyes; moreover, these adsorbents can be the solution for treatment of effluents colored by dyes or pigments after increasing its performance [16, 17].

Clays are strong adsorbents and have been used for decades [18]. Qualities such as chemical and mechanical stability, layered structure, ready availability and low cost make them an excellent adsorbent for the prevailing environmental pollution challenge [19, 20]. Their adsorption potential/efficiency largely depends on the surface area as well as on exchange capacity [21].

Kaolin is a soft white mineral that has a large array of uses. In its natural state, Kaolin is a white and soft powder, principally consisting of mineral kaolinite, which, under the electron microscope, is observed as roughly hexagonal, platy crystals ranging in size from about 0.1 micrometer to 10 micrometers [22].

The aim of this work was to evaluate the efficiency of Kaolin as a low-cost adsorbent to remove the Direct Blue 71 (DB71) dye from aqueous solutions. The effect of contact time, adsorbent dosage, particle size, and initial DB71 concentration at fixed temperature and pH was studied to find the optimum condition of DB71 dye removal.

2. Materials and Methods

The natural Kaolin clay samples were obtained from Sigma Aldrich (Darmstadt, Germany). Dirts and other unwanted materials were removed. The natural Kaolin clay was crushed, grinded, oven dried and sieved using the Tyler screen standard sieve of various sizes (4-80 mesh).

2.1. Preparation of Adsorbate

The Direct Blue 71 dye (CAS Number 4399-55-7, $C_{40}H_{28}N_7NaO_{13}S_4$, molecular weight of 965.94 g/mol) used in this study was obtained from Sigma Aldrich (Darmstadt, Germany); the chemical structure of this dye is shown in Figure 1.

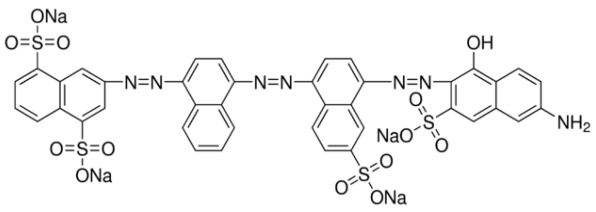

Figure 1: The structure of Direct Blue 71

All the chemicals used were of analytical reagent grade. To prepare a dye solution, 1 g of dye powder was dissolved in 1 L of distilled water to obtain the concentration of a stock solution with 1000 mg/L. Stock solution diluted to obtain the required concentrations range (10-100) mg/L in the experiments [8].

2.2. Adsorption Procedure

For each experimental run, 0.25 g of raw Kaolin (RK) powder with particle size was 75 μm added to 100 mL conical flask; then, 25 mL of the dye aqueous solution (10 mg/L) was added and the flask was tightly closed. These flasks were shaken at 200 rpm (Centric 400R model) at room temperature for a predetermined contact time. After that, they were centrifuged at 3000 rpm for 10 min. The pH of the solutions in all the adsorption processes was adjusted by adding 0.1 mol/L NaOH or 0.1 mol/L HCL (7). The dye concentration in the aqueous phase was determined by a UV spectrophotometer at (λ_{max}= 576 nm). The removal percentage (%R) of dye was calculated by the following equation (15):

$$\% R = \left[\frac{C_0 - C_e}{C_e}\right] \times 100 \quad (1)$$

C_0 (mg/L) and Ce (mg/L) are the concentrations of DB71 in the initial solution and at equilibrium. The adsorption capacity (q_e) of dye by the R_K adsorbent (mg/g) was calculated using the following equation (15):

$$q_e = \left[\frac{C_0 - C_e}{m}\right] V \quad (2)$$

Where, q_e (mg/g) is the amount of dye (mg) adsorbed onto a unit mass of the Kaolin (g) at equilibrium; C_0 (mg/L) and C_e (mg/L) are the concentrations of DB71 in the initial solution and at equilibrium; m (g) is the amount of adsorbent used V (L) is the volume of dye solution.

3. Results and Discussion

3.1. Characterization of Raw Kaolin (RK)

The specific surface area and porosity are the foremost characteristics of adsorbents. In the present study, the specific surface area and pore volume were estimated at 39.4 m^2/g and 0.036 ml/g, respectively. The SEM image of RK (Figure 2) showed an unevenly distributed cloudlike nature with hollows and pores.

3.2. Effect of Contact Time

The effect of contact time on removal of dye was studied and is shown in Figure 3. This figure indicates that the dye concentration in aqueous solutions rapidly decreases at the beginning and remains almost constant after 75 min; this is attributed to the large surface area of the adsorbent existing at the beginning of adsorption [23]. Moreover, the fast adsorption at the initial stage was due to the existence of large amount of adsorption sites. Thus, the progressive decrease of adsorption sites resulted in a slower adsorption reaction [24].

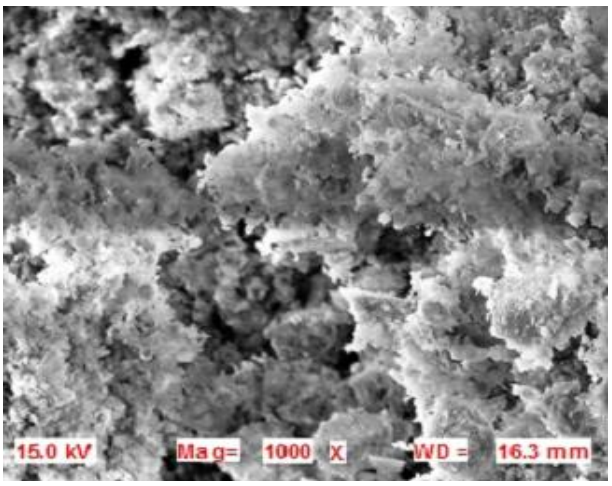

Figure 2: The SEM micrograph of RK

3.2. Effect of Contact Time

The effect of contact time on removal of dye was studied and is shown in Figure 3. This figure indicates that the dye concentration in aqueous solutions rapidly decreases at the beginning and remains almost constant after 75 min; this is attributed to the large surface area of the adsorbent existing at the beginning of adsorption [23]. Moreover, the fast adsorption at the initial stage was due to the existence of large amount of adsorption sites. Thus, the progressive decrease of adsorption sites resulted in a slower adsorption reaction [24].

3.3. Effect of Adsorbent Dosage

The effect of adsorbent dosage on the removal of the DB71 dye was studied and is shown in Figure 4. As shown in the figure, an increase was observed in the removal percentage of the DB71 dye with the increase of adsorbent dose until it asymptotically reached 98.5%. This may be due to an increase in the availability of surface active sites with the increase of the dose [25].

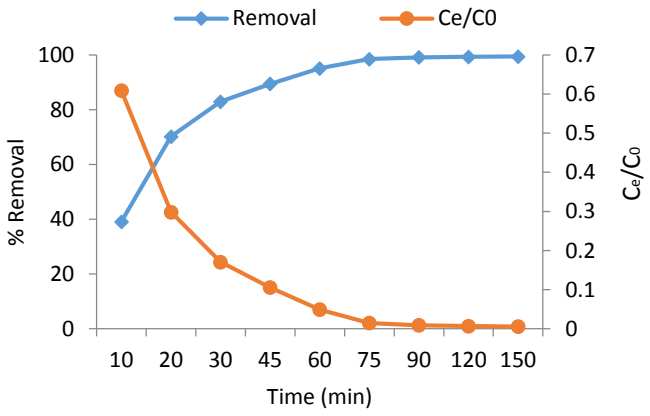

Figure 3: Effect of contact time on the removal percentage of DB71 dye onto RK (C_0 = 100 mg/L, Adsorbent dosage 2 g/L, pH = 7, temp= 25 ± 2 ^{0}C and particle size 10 mesh)

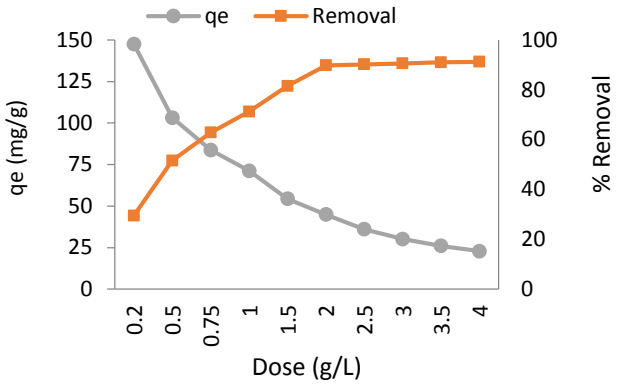

Figure 4: The effect of adsorbent dosage on removal percentage of the DB71 dye onto RK (C_0 = 100 mg/L, Contact time 75 min, pH = 7, temp= 25 ± 2 ^{0}C and particle size 10 mesh)

3.4. Effect of Particle Size

Adsorption of the DB71 dye was studied on five particle sizes of adsorbent. The results are shown in Figure 5. It was observed from Figure 5 that the dye percentage removal decreased with increasing the particle size of the adsorbent. The decrease in particle size led to an increase of available active sites on the surface of the adsorbent and, consequently, an increase in the adsorption process on the RK surface due to the high surface area [26, 27]. Furthermore, the diffusional resistance to mass transfer increased by increasing particle size the beginning of adsorption [23]. Moreover, the fast adsorption at the initial stage was due to the existence of large amount of adsorption sites.

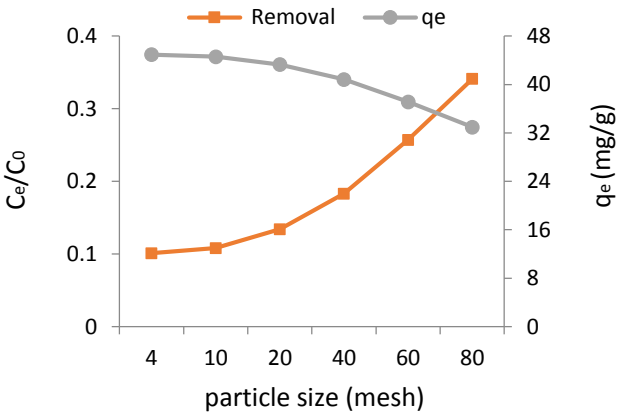

Figure 5: The effect of particle size on removal percentage of the DB71 dye onto RK at (C_0 = 100 mg/L, Contact time 75 min, pH = 7, temp= 25± 2 ^{0}C and Adsorbent dosage 2 g/L)

3.5. Adsorption Isotherm Models

For the design of adsorption systems, adsorption isotherm models are very important. This tool provides useful information regarding maximum adsorption capacity and the expected interactions between adsorbates and adsorbents. Here, four isotherm models, i.e., Langmuir, Freundlich, Dubinin–Radushkevich (D–R), and Temkin, were applied to evaluate equilibrium experimental data. The Langmuir

isotherm elaborates on the formation of monolayer adsorption of molecules due to all the binding sites showing an equal affinity for sorbate molecules. Equation 3 represents the linear form for the Langmuir isotherm [28]:

$$\frac{Ce}{q_e} = \frac{1}{q_m K_L} + \frac{C_e}{q_m} \quad (3)$$

where C_e is the concentration of DB71 at equilibrium (mg/L), q_e is the adsorption capacity (mg/g), qm represents the maximum adsorption capacity (mg/g) , and K_L is the Langmuir isotherm constant [24]:

$$R_L = \frac{1}{1+K_L C_0} \quad (4)$$

C_0 (mg/L) is the concentrations of dye in the initial solution.

The separation factor (R_L) is a dimensionless equilibrium parameter which may be used to calculate favorability of the adsorption process from the expression.

$R_L = 0$ is irreversible isotherm
$R_L = 1$ is linear isotherm
$R_L > 1$ is unfavorable isotherm

$0 < R_L < 1$ is favorable isothermThe heterogeneous surfaces adsorption is mainly determined using the Freundlich isotherm which tells about the adsorption sites of different attraction. Using the linear form in Eq. (5), this isotherm could be assessed as [20]:

$$\text{Log } q_e = \frac{1}{n} \log C_e + \log K_F \quad (5)$$

where C_e is the concentration at equilibrium (mg/L), K_F denotes multilayer adsorption capacity, and (1/n) is the intensity of adsorption.

Dubinin–Radushkevich (D-R) (Eqs. 6 and 7) is known to be more generalized than the Langmuir isotherm; it easily distinguishes the physicochemical adsorption process because it is not dependent on ideal assumptions, e.g., absence of steric hindrances between adsorbates and incoming particles, surface homogeneity on microscopic level, and equipotential of adsorption sites [29]:

$$\text{Ln } q_e = \text{Ln } q_m - K\varepsilon^2 \quad (6)$$

$$\varepsilon = RT \text{ Ln } (1+\frac{1}{C_e}) \quad (7)$$

The difference between saturated liquid phase and frequently adsorbate phase is known as adsorption potential, as proposed by Polanyi. The total specific micropore volume of the adsorbent is represented by q_m (saturation limit). Equation 8 is applied to calculate the mean free energy E (kJ/mol).

$$E = \frac{1}{\sqrt{2B}} \quad (8)$$

If the activation energy E < 8 KJ/mol, the adsorption process is physisorption and if E is in between 8-16 KJ/mol, the process is chemisorptions in nature.

The relationship between adsorbent–adsorbate interactions on surfaces and heat of adsorption is well described by the Temkin equation. It suggests that heat of adsorption of all molecules decreased linearly with completion of adsorption sites in the adsorbent. Equation 9 is the Temkin isotherm which is given below [24]:

$$q_e = B \text{ Ln } A + B \text{ Ln } Ce \qquad B = (RT)/b \quad (9)$$

Table 1 shows the values of adsorption constants of all the models which give an idea concerning the favorability and unfavorability of the process. The plot of C_e/C_0 versus C_e (this Figure is not shown), yielded a straight line, indicating that the experimental data tabulated in Table 1 appeared to follow the Langmuir isotherm. Moreover, the calculated values of R_L were less than 1 at all the concentrations, which also represented the favorable adsorption of DB71 onto R_K.

The Freundlich isotherm equation was applied to validate the adsorption of DB71; as a result, a linear plot was obtained. The calculated values of adsorption intensity (1/n) were greater than 0 and less than 1, indicating the favorability of the adsorption. The regression coefficient R2 = 0.884 gave validation of experimental data. The adsorption intensity of the Freundlich constant (n) was found to be 2.65; the n value did not lie in the 1-10 range, indicating the favorable adsorption.

A plot of Ln Cads versus ε^2 (this Figure is not shown), yielded a straight line; from the slope and intercept, β and qm values were calculated, respectively (Table 1). The magnitude of free energy (E) plays an important role in evaluating the kind of adsorption. Hence, in this case, the value of E was 3.25 kJ/mol pertaining to the applicability of experimental data for the D–R isotherm and it described that the process was physio-adsorption in nature.

Furthermore, Table 1 also shows the comparison of R^2 of all the isotherms. The favorability order on the basis of regression coefficients is as follows: Langmuir ($R^2 = 0.995$) > D-R ($R^2 = 0.912$) > Freundlich ($R^2 = 0.884$) > Temkin ($R^2 = 0.824$).

Therefore, each isotherm has appropriate merits in describing the potential of FK for the adsorption of DB71. The values of the correlation coefficient indicated that the adsorption process was compatible, feasible and experimental data followed the D–R and Langmuir isotherm models. Table 2 shows a comparison between the adsorption capacities of the F_K adsorbent used in this work with other adsorbents reported in the literature.

Table 1: Data of the various isotherms tabulated with various parameters

Langmuir				Freundlich			D-R			Temkin		
q_e	R_L	K_L	R^2	K_F	n	R^2	q_m	E	R^2	B	A	R^2
48.2	0.51	0.189	0.995	1.725	2.65	0.884	29.16	3.25	0.912	36.41	8.24	0.824

3.6. Adsorption Kinetic Models

The kinetic study for the adsorption of DB71 on to the FK was carried out at a fixed initial concentration to investigate the controlling mechanism as a function of different concentration, i.e., 10-100 mg/L. This parameter is important for evaluating the adsorption phenomenon followed by sorbate molecules to attach on the adsorbent surface. In order to evaluate the adsorption kinetics, the effect of agitation time was observed from 10 to 150 min. In kinetic study, the rate of adsorption of DB71 onto FK was determined by using different kinetic models such as pseudo-first-order kinetic, pseudo-second-order kinetic and diffusion models. The pseudo-first-order and second-order kinetic equations are given as Eqs. (10) and (11), respectively [30]:

$$\text{Log } (qe - qt) = \log qe - \frac{K_1}{2.303}t \quad (10)$$

$$\frac{t}{q_t} = \frac{1}{k_2 qe^2} + \frac{1}{qe\, t} \quad (11)$$

q_e and q_t are the amount of dye adsorbate on the adsorbent (mg/g) at equilibrium and the time t, respectively, and K_1 (1/min) and K_2 (g/mol/min) are the adsorption rate constants. Q_e, K_1, and K_2 were obtained from the slope and intercept of the linear plots of (q_e - q_t) versus t and t/qt versus t (this Figure is not shown).

Kinetic parameters along with correlation coefficients of kinetic models are given in Table 3. It is noted that R^2 values of the pseudo-first-order kinetic model at different concentrations may not well explain the kinetics of adsorption whereas the pseudo-second-order explain the kinetics of adsorption whereas the pseudo-second-order model R^2 values better explain the adsorption manner relative to the former one. The later one describes the rate-limiting step as physical adsorption based on physical interaction of adsorbate-adsorbent molecules. Moreover, the pseudo-second-order kinetic model describes adsorption as purely physical in nature as supported by physical interaction between DB71 and FK. Both the kinetic models do not recognize the diffusion mechanism; hence, kinetic results were evaluated with diffusion models [26]:

$$q_t = K_d\, t^{0.5} + C \quad (12)$$

Here, q_t is the adsorbed concentration at the time t, while K_d is known as the intra-particle diffusion rate constant. From the linear plot of qt versus $t^{1/2}$ (this Figure is not shown), it was observed that lines did not pass the origin, suggesting that for adsorption of DB71 onto FK, the intra-particle diffusion was not only the rate-limiting step and some degree of boundary layers also controlled the process.

Table 2: Comparison of maximum adsorption capacities of dye by various adsorbents

Adsorbent	q_e (mg/g)	Ref	Adsorbent	q_e (mg/g)	Ref
A. filiculoides	31.7	[3]	Bentonite	27.6	[11]
Tea waste	29.2	[4]	Bagasse pith	19.8	[15]
Fruit waste	27.1	[6]	Lemna minor	26.9	[21]
Chitosan	34.2	[28]	Sepiolite	24.8	[24]

Table 3: A comparison of various kinetics at different initial DB71concentrations

DB71 Concentration (mg/L)	$(q_e)_{exp}$	Intraparticle diffusion model			Pseudo-first order			Pseudo-second order		
		K_d	C	R^2	$(q_e)_{cal}$	K	R^2	$(q_e)_{cal}$	K	R^2
10	4.72	0.619	7.142	0.804	1.912	0.141	0.845	4.523	0.0295	0.996
25	12.31	0.484	5.113	0.817	5.391	0.119	0.864	11.25	0.0176	0.994
50	23.31	0.395	3.726	0.796	11.25	0.084	0.812	21.72	0.0096	0.998
100	44.91	0.246	1.864	0.809	19.25	0.069	0.835	41.86	0.0079	0.999

4. Conclusion

In our study, RK as an adsorbent had a high potential for removing of the DB71 dye from the aqueous solution. The kinetics of the DB71 adsorption was examined by using the pseudo-first order and pseudo-second order and diffusion kinetic models under different conditions. The results of adsorption kinetic of the DB71 dye in the aqueous solution followed the pseudo-second order model. Moreover, the data were evaluated by using the Langmuir, Freundlich, D-R, and Temkin models. The values of the correlation coefficient indicated that the adsorption process was compatible and feasible and also the experimental data followed the D-R and Langmuir isotherm models.

Authors' Contributions

D.B., and M.D., study design; M.Z. and M.S., field work; data analysis, and drafting of the manuscript.

Conflict of Interest

We are grateful to the student research committee of the Zahedan University of Medical Sciences for their financial

supports (Project No. 9263).

References

1. Afkhami A, Saber-Tehrani M, Bagheri H. Modified Maghemite Nanoparticles as an Efficient Adsorbent for Removing some Cationic dyes from Aqueous Solution. *Desalination*. 2010; 263: 240-8.
2. Yousuf M, Mollah A, Gomes JA, Das KK, Cocke DL. Electrochemical Treatment of OrangeII Dye Solution-use of Aluminum Sacrificial Electrodes and Floc Characterization. *J Hazard Mater*. 2010; 174: 851-8.
3. Balarak D, Mahdavi Y. Experimental and Kinetic Studies on Acid Red 88 Dye (AR88) Adsorption by Azolla Filiculoides. *Biochem & Physiol*. 2016; 5(1): 1-5.
4. Uddin MT, Islam MA, Mahmud S, Rukanuzzaman M. Adsorptive Removal of Methylene Blue by Tea Waste. *J Hazard Mater*. 2009; 164: 53-60.
5. Gao H, Zhao S, Cheng X, Wang X, Zheng L. Removal of Anionic azo Dyes from Aqueous Solution Using Magnetic Polymer Multi-Wall Carbon Nanotubes Nanocomposite as Adsorbent. *Chem Eng J*. 2013. 223: 84-90.
6. Pavan FA, Lima EC, SDias SLP, Mazzocato AC. Methylene Blue Biosorption from Aqueous Solutions by Yellow Passion Fruit Waste. *J Hazard Mater*. 2008; 150: 703-12.
7. Balarak D, Jaafari J, Hassani G, Mahdavi Y, Tyagi I, Agarwal S, Gupta VK. The Use of Low-Cost Adsorbent (Canola Residues) for the Adsorption of Methylene Blue from Aqueous Solution: Isotherm, Kinetic and Thermodynamic Studies. *Colloids and Interface Sci Commun*. 2015; 7: 16-9.
8. Kuo CY, Wu CH, Wu JY. Adsorption of Direct dyes from Aqueous Solutions by Carbon Nanotubes: Determination of Equilibrium, Kinetics and Thermodynamics Parameters. *J Colloid Interface Sci*. 2008; 327(2): 308-15.
9. Assadi A, Soudavari A, Mohammadian M. Comparison of Electrocoagulation and Chemical Coagulation Processes in Removing Reactive red 196 from Aqueous Solution. *J Hum Environ Health Promot*. 2016; 1 (3): 172-82.
10. Deniz F, Karaman S. Removal of Basic Red 46 Dye from Aqueous Solution by Pine Tree Leaves. *Chem Eng J*. 2011; 170(1): 67-74.
11. Gök Ö, Özcan AS, Özcan A. Adsorption Behavior of a Textile Dye of Reactive Blue 19 from Aqueous Solutions onto Modified bentonite. *Appl Surf Sci*. 2010; 256(17): 5439-43.
12. Balarak D, Joghataei A, Azadi NA, Sadeghi S. Biosorption of Acid Blue 225 from Aqueous Solution by Azolla Filiculoides: Kinetic and Equilibrium Studies. *Am Chem Sci J*. 2016; 12 (2): 1-10.
13. Akar T, Ozcan AS, Tunali S, Ozcan A. Biosorption of a Textile Dye (Acid Blue 40) by Cone Biomass of Thuja Orientalis: Estimation of Equilibrium, Thermodynamic and Kinetic Parameters. *Bioresour Technol*. 2008; 99(8): 3057-65.
14. Arami M, Limaee NY, Mahmoodi NM. Evaluation of the Adsorption Kinetics and Equilibrium for the Potential Removal of Acid Dyes Using a Biosorbent. *Chem Eng J*. 2008; 139(1): 2-10.
15. Amin NK. Removal of Reactive dye from Aqueous Solutions by Adsorption onto Activated Carbons Prepared from Sugarcane Bagasse Pith. *Desalination*. 2008; 223(1-3): 152-61.
16. Galán J, Rodríguez A, Gómez JM, Allen SJ, Walker GM. Reactive Dye Adsorption onto a Novel Mesoporous Carbon. *Chem Eng J*. 2013; 219: 62-8.
17. Padmesh TVN, Vijayaraghavan K, Sekaran G, Velan M. Application of Azolla Rongpong on Biosorption of Acid Red 88, Acid Green 3, Acid Orange 7 and Acid Blue 15 from Synthetic Solutions. *Chem Eng J*. 2006; 122(1–2): 55-63.
18. Luo P, Zhao Y, Zhang B, Liu J, Yang Y, Liu J. Study on the Adsorption of Neutral Red from Aqueous Solution onto Halloysite Nanotubes. *Water Res*. 2010; 44: 1489-97.
19. Moussavi G, Mahmoudi M. Removal of azo and Anthraquinone Reactive Dyes from Industrial Wastewaters Using MgO Nanoparticles. *J Hazard Mater*. 2009; 168: 806-12.
20. Li Z, Schulz L, Ackley C, Fenske N. Adsorption of Tetracycline on Kaolinite with PH-Dependent Surface Charges. *J Colloid Interface Sci*. 2010; 351(1): 254-60.
21. Balarak D, Mahdavi Y, Kord Mostafapour F, Joghataei A. Batch Removal of Acid Blue 292 Dye by Biosorption onto Lemna minor: Equilibrium and Kinetic Studies. *J Hum Environ Health Promot.* 2016; 2(1): 9-19.
22. Inyinbor AA, Adekola FA, Olatunji GA. Kinetics, Isotherms and Thermodynamic Modeling of Liquid Phase Adsorption of Rhodamine B Dye onto Raphia Hookerie Fruit Epicarp. *Water Resour and Ind*. 2016; 15: 14-27.
23. Muthukumaran C, Sivakumar VM, Thirumarimurugan M. Adsorption Isotherms and Kinetic Studies of Crystal Violet Dye Removal from Aqueous Solution Using Surfactant Modified Magnetic Nanoadsorbent. *J Taiwan Inst of Chem Eng*. 2010; 63: 354-62.
24. Eren E, Cubuk O, Ciftci, H, Eren B, Caglar B. Adsorption of Basic dye from Aqueous Solutions by Modified Sepiolite: Equilibrium, Kinetics and Thermodynamics Study. *Desalination*. 2010; 252: 88-96.
25. Ozcan A, Ozcan AS. Adsorption of Acid Red 57 from Aqueous Solutions onto Surfactant-modified Sepiolite. *J Hazard Mater*. 2005; B125: 252-9.
26. Balarak D, Dashtizadeh M, Abasizade H, Baniasadi M. Isotherm and Kinetic Evaluation of Acid Blue 80 Dye Adsorption on Surfactant-Modified Bentonite. *J Hum Environ Health Promot*. 2018; 4 (2) :75-80.
27. Moussavi SP, Mohammadian Fazli M. Acid Violet 17 Dye Decolorization by Multi-walled Carbon Nanotubes from Aqueous Solution. *J Hum Environ Health Promot*. 2016; 1(2): 110-7.
28. Rasoulifard MH, Taheri Qazvini N, Farhangnia E, Heidari A, Doust Mohamad MM. Removal of Direct Yellow 9 and Reactive Orange 122 from Contaminated Water Using Chitosan as a Polymeric Bioadsorbent by Adsorption Process. *J Color Sci Technol*. 2010; 4: 17-23.
29. Crini G, Badot PM. Application of Chitosan, a Natural Aminopolysaccharide, for Dye Removal from Aqueous Solutions by Adsorption Processes Using batch Studies: A Review of Recent Literature. *Prog Polym Sci*. 2008; 33(4): 399-447.
30. Baocheng QU, Jiti ZH, Xiang X, Zheng C, Hongxia ZH, Xiaobai ZH. Adsorption Behavior of Azo Dye CI Acid Red 14 in Aqueous Solution on Surface Soils. *J Environ Sci*. 2008; 20(6): 704-9.